

Studies on microstructure, mechanical and corrosion properties of high nitrogen stainless steel shielded metal arc welds

Raffi Mohammed¹, Madhusudhan Reddy G³, and Srinivasa Rao K²

¹ Department of Metallurgical & Materials Engineering, NIT - Andhra Pradesh, India

² Department of Metallurgical Engineering, Andhra University, Visakhapatnam, India

³ Defence Metallurgical Research Laboratory, Hyderabad, India.

Corresponding author: raffia.u@gmail.com

Abstract

The present work is aimed at studying the microstructure, mechanical and corrosion properties of high nitrogen stainless steel shielded metal arc (SMA) welds made with Cromang-N electrode. Basis for selecting this electrode is to increase the solubility of nitrogen in weld metal due to high chromium and manganese content. Microstructures of the welds were characterized using optical microscopy (OM), field emission scanning electron microscopy (FESEM) and electron back scattered diffraction (EBSD) mainly to determine the morphology, phase analysis, grain size and orientation image mapping. Hardness, tensile and ductility bend tests were carried out to determine mechanical properties. Potentio-dynamic polarization testing was carried out to study the pitting corrosion resistance using a GillAC basic electrochemical system. Constant load type testing was carried out to study stress corrosion cracking (SCC) behaviour of welds. The investigation results shown that the selected Cr-Mn-N type electrode resulted in favourable microstructure and completely solidified as single phase coarse austenite. Mechanical properties of SMA welds are found to be inferior when compared to that of base metal and is due to coarse and dendritic structure.

1. Introduction

Austenitic stainless steels are used due to its excellent corrosion resistance with good formability and weldability. The development of austenitic stainless steel with improved properties was initiated and became widespread in the nineteenth century [1]. Generally austenitic stainless steels contain chromium and nickel as major alloying element and nickel is used to stabilize the austenitic phase and provide corrosion resistance to some extent [2]. Earlier research was focussed on improvements related to increase in chromium, molybdenum and nickel contents [3]. Now a day's more interest has been identified in raising the level of dissolved nitrogen in the steel and further it led to the development of high nitrogen austenitic stainless steel (HNS) with nitrogen levels about 0.5 wt%. Addition of nitrogen has resulted in austenitic stainless steel with an excellent combination of mechanical properties and corrosion resistance. Nitrogen is one of the important alloying elements which may be used to replace the Ni addition. It is having the advantages of increasing the pitting corrosion resistance and enhances the strength of the steel. Nickel free high nitrogen austenitic stainless steel is having wide scope in armoured structures in defence applications. Due to its low cost, high strength, ductility and toughness along with superior localized corrosion resistance, it can be recommended to replace existing armour grade high strength low alloy steels. In fabricating the structural material, welding is one of the commonly used fabrication technique for joining high



nitrogen austenitic stainless steels. Nitrogen desorption during fusion welding which could result in lowering the mechanical properties and corrosion resistance. Nitrogen induced porosity can be reduced by keeping the enough solubility of high nitrogen in the weld metal. Defects like porosity and solidification cracking can be overcome by the use of matching filler wire/electrode which produces required amount of delta ferrite in the weld metal. During welding, it requires special care to ensure that the nitrogen remains in the weld metal [4]. Based on industrial practice, the weld metal should contain a desirable ferrite level in stainless steel welds [5]. During solidification in welding, if the nitrogen level exceeds limit of solubility the nitrogen bubbles can form in the liquid, thereby increases the possibility for nitrogen induced porosity [6]. To avoid the problem of nitrogen-induced porosity, the solubility of nitrogen in the weld metal has to be high enough to accommodate any increase in nitrogen concentration. Higher levels of chromium and manganese are desired in the weld metal when filler wires for welding are selected to increase the solubility limit of nitrogen in austenitic stainless steel. To minimize the hot cracking tendency, choosing a filler wire with low impurity levels (e.g. S, P) with minimizing the degree of segregation of the major alloying elements and the level of intermetallic phases in the weld metal [7]. Nitrogen alloying in the filler wire may also play a vital role in controlling the precipitation of intermetallic compounds [8], by raising the transformation temperature of ferrite/austenite and assisting the formation of austenite phase in heat affected zone of a stainless steel weld. Generally, stainless steels are susceptible to localized corrosion such as pitting and stress corrosion cracking (SCC) in chloride containing environment. SCC is due to the simultaneous action of aggressive environment, tensile stress and susceptible microstructure [9]. Welding may alter the favourable microstructure and sensitive to pitting and stress corrosion cracking. Commercially matching filler wires similar to the composition of the base metal (HNS) are not presently available. In view of the above problems, authors made an attempt to study the shielded metal arc welds of high nitrogen austenitic stainless steel using a nearest matching of Cromang-N steel electrode. Aim of the present work is to investigate the microstructural changes and correlate them with mechanical and corrosion behaviour of welds.

2. Experimental Details

High nitrogen austenitic stainless steel (HNS) plates of size (500mmx150mmx5mm) were joined with near matching electrode (17Cr-17Mn-0.36N) type using SMAW process. Schematic diagram of joint geometry with dimensions are given in Fig.1. A set of plates were single-V butt welded using shielded metal arc welding (SMAW) with an electrode of Cromang-N steel (17Cr-17Mn-0.36N) was chosen in present investigation and is shown in Fig.2. The composition of the base metal and electrode are given in the Table 1. The welding parameters, such as welding current and welding speed, were optimized after having several experiments through many welding trials and obtained a sound welds free from defects. The optimized welding parameters are given in Table 2. Phases were analysed using X-Ray diffraction technique. Microstructure studies were characterized at various zones of the welds using optical microscopy, field emission scanning electron microscopy (FESEM). Orientation imaging microscope (OIM) studies were done to find the orientation of the grains and the amount of different phases in the various zones of weldment using electron back-scattered diffraction (EBSD) method. Microhardness values were recorded towards the longitudinal directions of the weld with a load of 0.5Kgf for 20 seconds as per ASTM E384-09 standards using Vickers hardness testing machine.

Tensile testing is carried out using a universal testing machine at room temperature as per ASTM-E8. Face bend testing of the material was conducted to observe the crack development to know the ductile nature of the weld as per ASTM E190-92. Pitting corrosion resistance of base metal and SMA welds were determined using potentiodynamic polarization testing in aerated 3.5%NaCl solution. Transverse tensile test specimens were extracted from the base metal (HNS) and SMA weld joint using wire-cut electric discharge machining. Stress corrosion cracking (SCC) testing was carried out using constant load type machine with applied stress of 50% yield strength and in 45% MgCl₂ solution boiling at 155°C as per ASTM G36.

Table 1 Chemical composition of the base metal and electrode

Material	Element (wt %)										
	C	Mn	Cr	N	S	P	Ni	Co	Mo	Si	Fe
Base Metal (HNS)	0.076	19.78	17.96	0.543	0.007	0.051	-	-	-	0.34	Bal.
Electrode (Cromang-N)	0.066	17.36	17.33	0.366	0.017	0.047	0.09	-	-	0.522	Bal.

Table 2 Optimized parameters for welding using shielded metal arc welding

Welding Current (A)	110-130
Welding Speed (mm/sec)	04
Electrode diameter/mm	3.2
Electrode position	45°
No. of passes	03
Root gap/mm	1.5

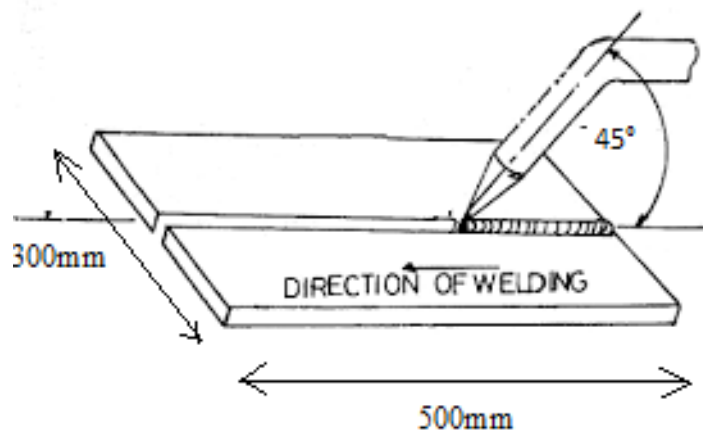


Fig.1 Schematic diagram of joint geometry with dimensions

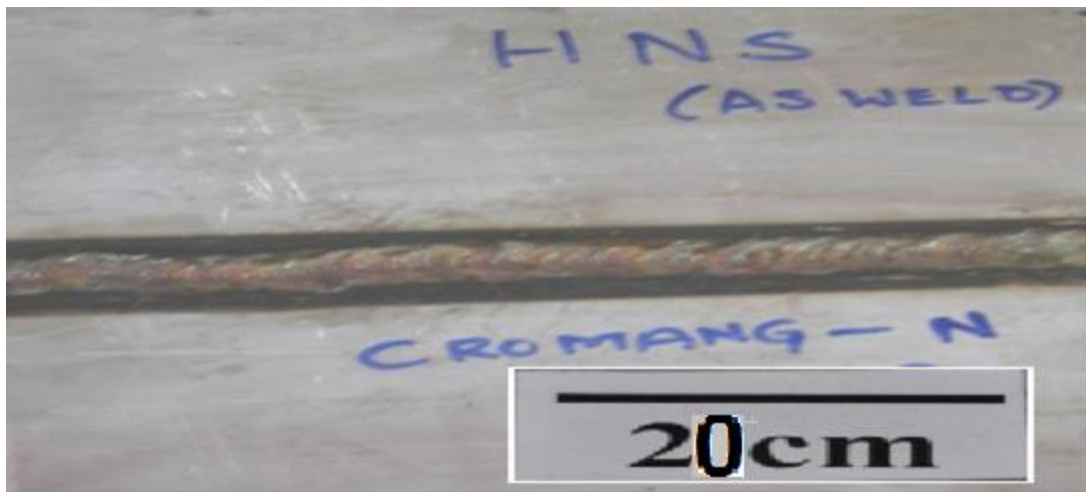


Fig.2 Shielded metal arc weld joint of high nitrogen steel

3. Results and Discussions

X-ray radiography of welds revealed no significant defects and observed to be a sound weld as shown in Fig. 3. Fig.4 shows the XRD results for base metal as well as for weldment. From the XRD patterns, there are numerous sharp peaks that correspond to the presence of austenite. The single phase identified in the base metal and whereas in the welds the presence of austenite and delta ferrite are observed which is very beneficial to avoid the cracking tendency.

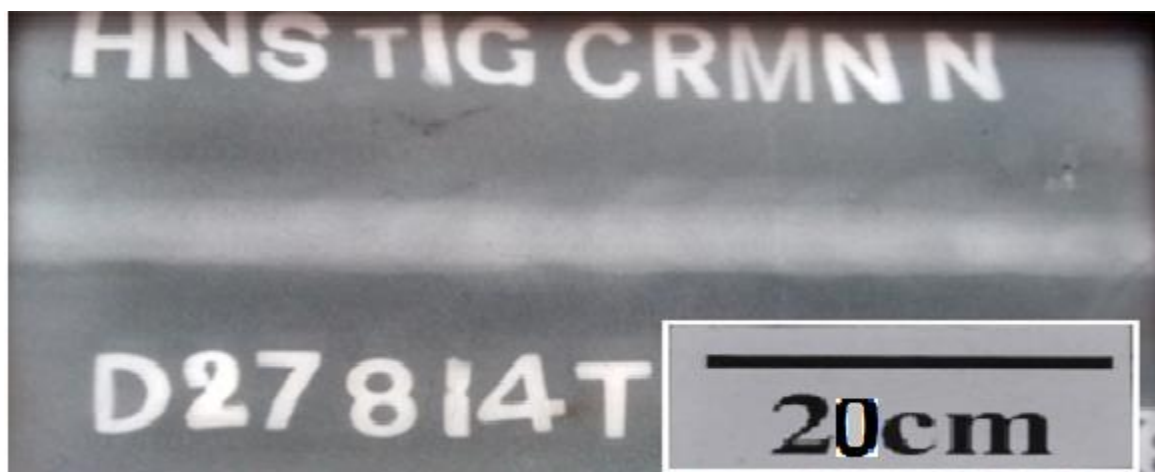


Fig.3 X-ray radiograph of SMA weld made with Cr-Mn-N electrode

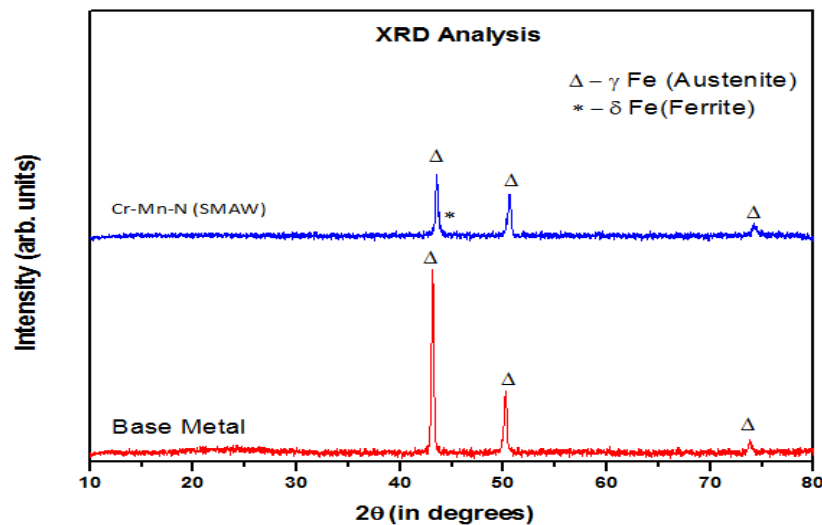


Fig.4 XRD analysis peaks of High nitrogen steel (base metal) and SMA welds

3.1 Microstructure

3.1.1 High nitrogen stainless steel

Optical and field emission scanning electron micrographs of the base metal is observed to have fine grains of austenite and annealing austenite twins and are shown in Fig. 5. In high nitrogen stainless steel, nitrogen acts as austenite stabilizer and effective in completely replacing nickel. Addition of chromium and manganese increase the solubility of nitrogen. Therefore, nitrogen content in Fe-Cr-Ni alloys are much lower than that in Fe-Cr-Mn alloys and other alloying elements like Ti, V, Nb and Zr enhance the solubility due to their high affinity for nitrogen.

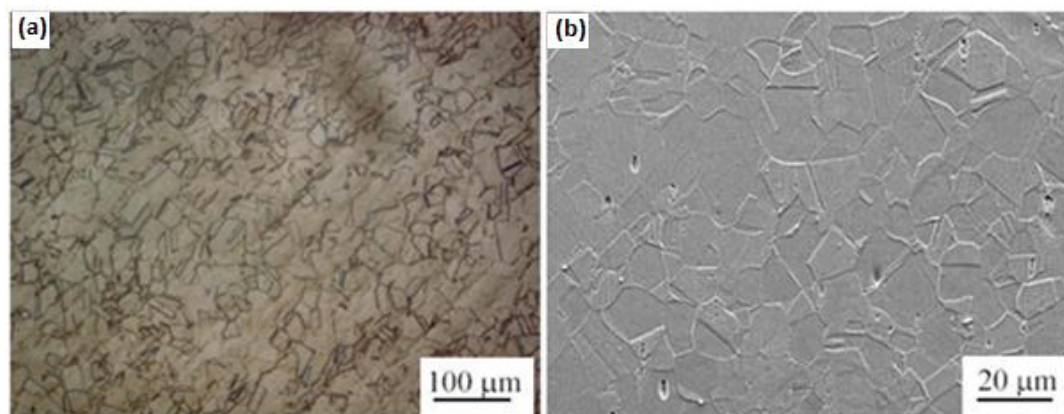


Fig. 5 Microstructure of base metal (high nitrogen stainless steel) (a) optical (b) field emission scanning electron micrograph

3.1.2 Shielded metal arc welds

Electrode composition (Cr-Mn-N) which is having high amount of chromium and manganese helps to improve the solubility of nitrogen in the weld metal. Fig. 6a shows the weld metal, weld interface and base metal regions at lower magnification of the high nitrogen stainless SMA welds. At the weld interface, along the fusion boundary towards the base metal transition of coarse grains to fine grains

are observed as shown in Fig.6b and having maximum austenite structure due to the dilution of adjacent base metal which is having nitrogen which is completely soluble in the solid solution. The weld metal microstructure is fully austenitic and consisted of coarse columnar austenite grains growing from the fusion boundary towards the weld centreline and it can be observed in Fig. 6c. The reduction of delta-ferrite during solidification and in the room temperature microstructure of the Cr-Mn-N weld is attributed to the presence of relatively higher amount of nitrogen and completely soluble due to the higher level of manganese content. Higher manganese level of this electrode may relieve the cracking tendency of the weld metal by combining with harmful elements such as sulphur to form inclusions [9]. No cracks or porosity were observed in any of the interface of the weld joints as shown in Fig.6b. Figs. 7-9 show the grain orientation maps and phase analysis maps of the base metal, fusion zone and welds interface of the high nitrogen stainless steel respectively. The observations from the colour codes obtained from orientation of grains having mis-orientation angle of 46° and OIM maps were random in nature in the base metal as observed in Fig.7 whereas in the fusion zone shown in Fig.8 coarse grains orientation and having mis-orientation angle of 28° . In weld interface, observed to be having coarse grains to fine grains transition from fusion zone to base metal and mis-orientation angle of 37° is shown in Fig.9. Different phases were analysed using phase maps and recorded the percentage of delta ferrite, austenite and also determined the distribution of the ferrite in the austenite matrix.

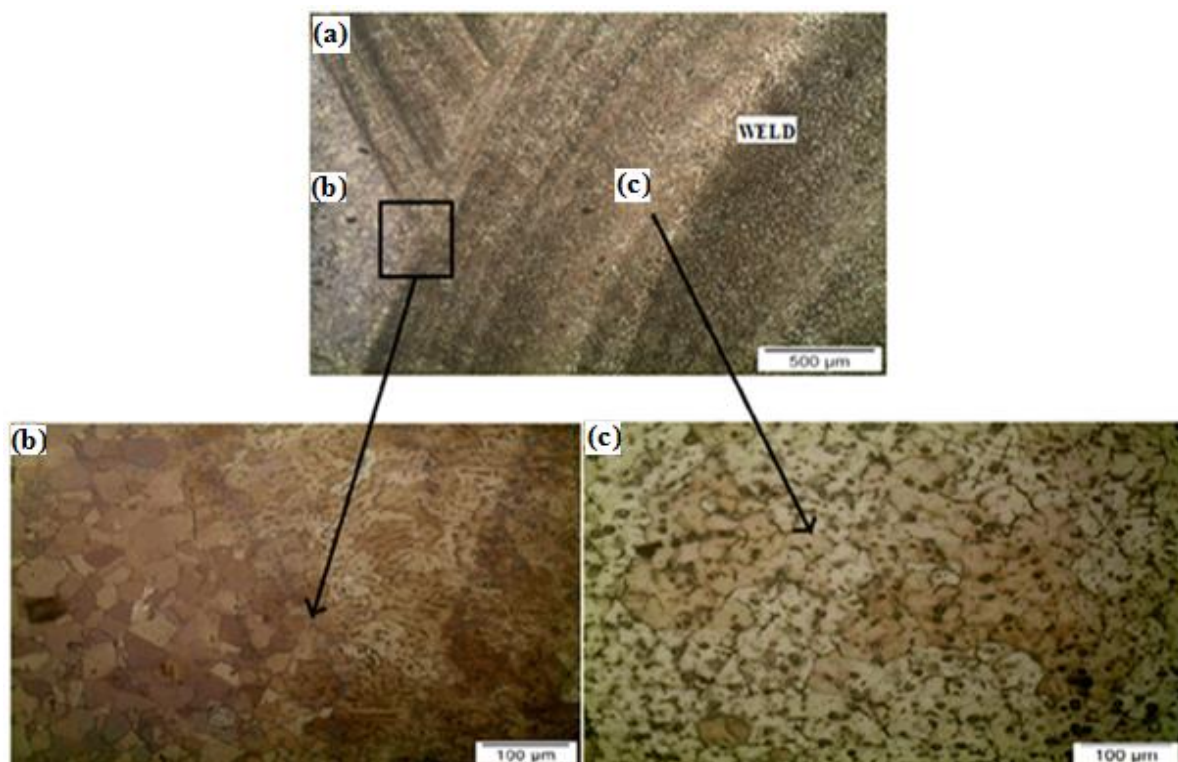


Fig.6 Optical micrographs of High nitrogen steel (a). Weld interface; (b). Heat affected zone; (c). Fusion zone

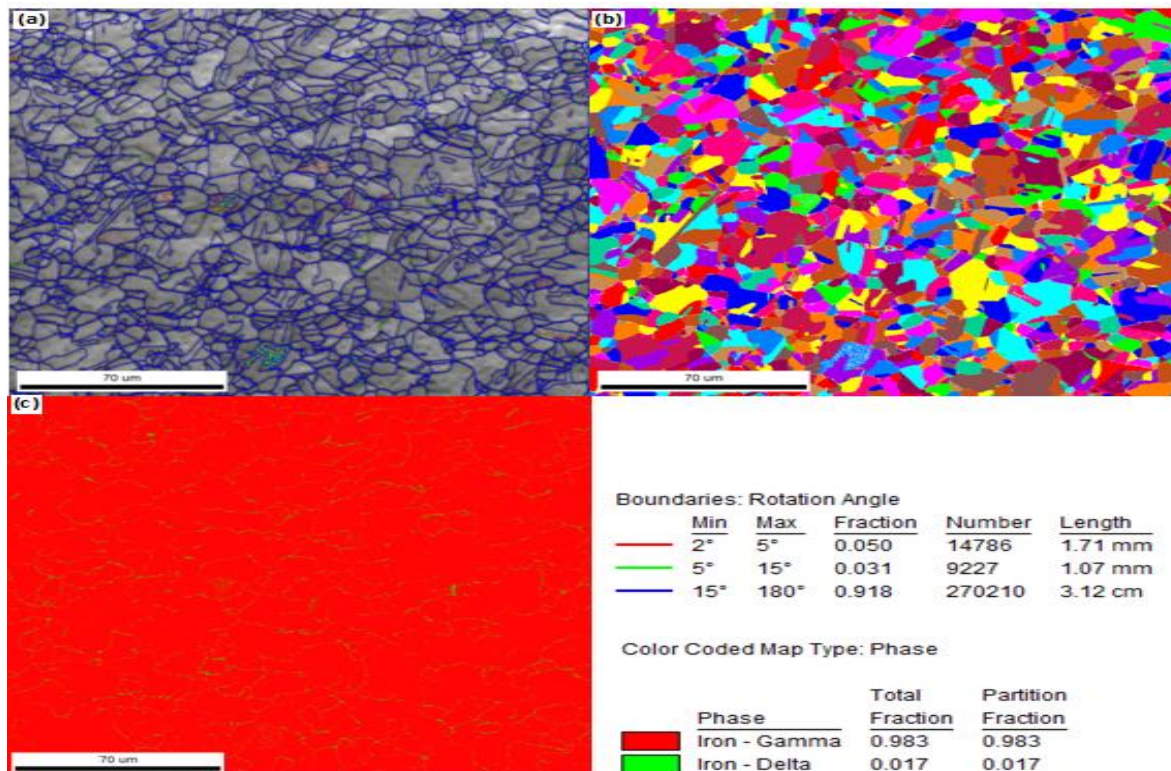


Fig.7 Grain orientation, OIM maps and phase analysis of high nitrogen stainless steel (Base Metal)

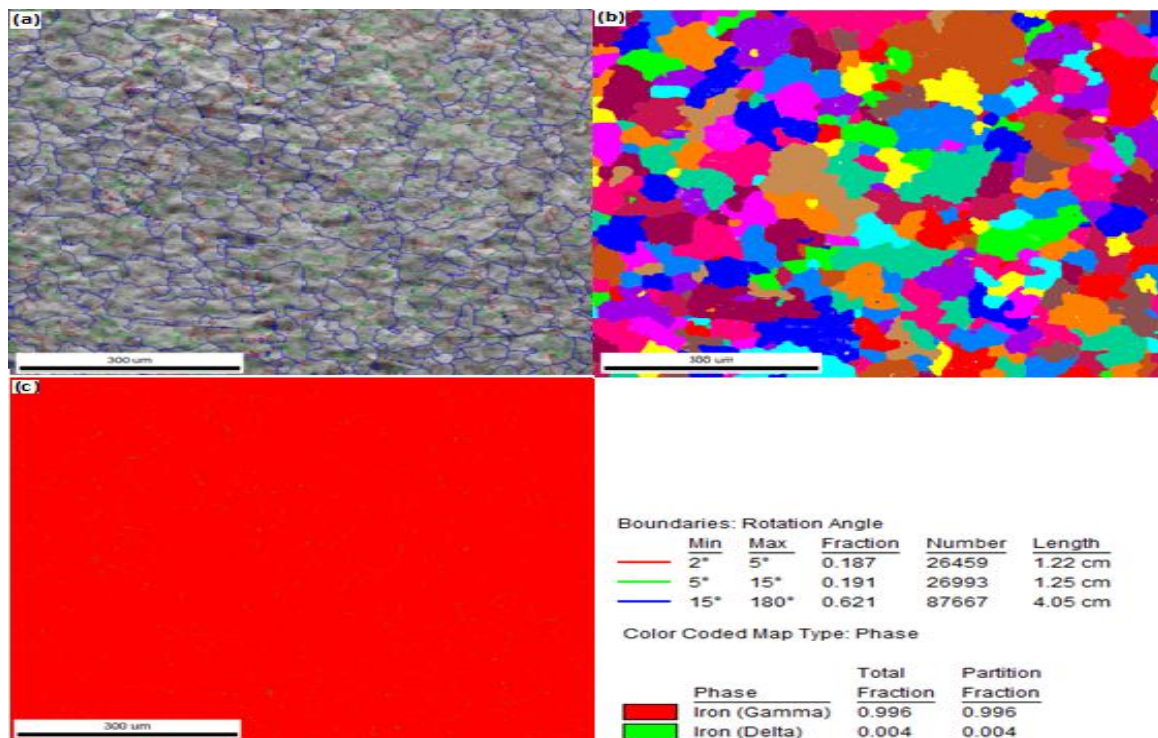


Fig.8 Grain orientation, OIM and phase analysis maps for fusion zone of high nitrogen stainless steel SMA welds

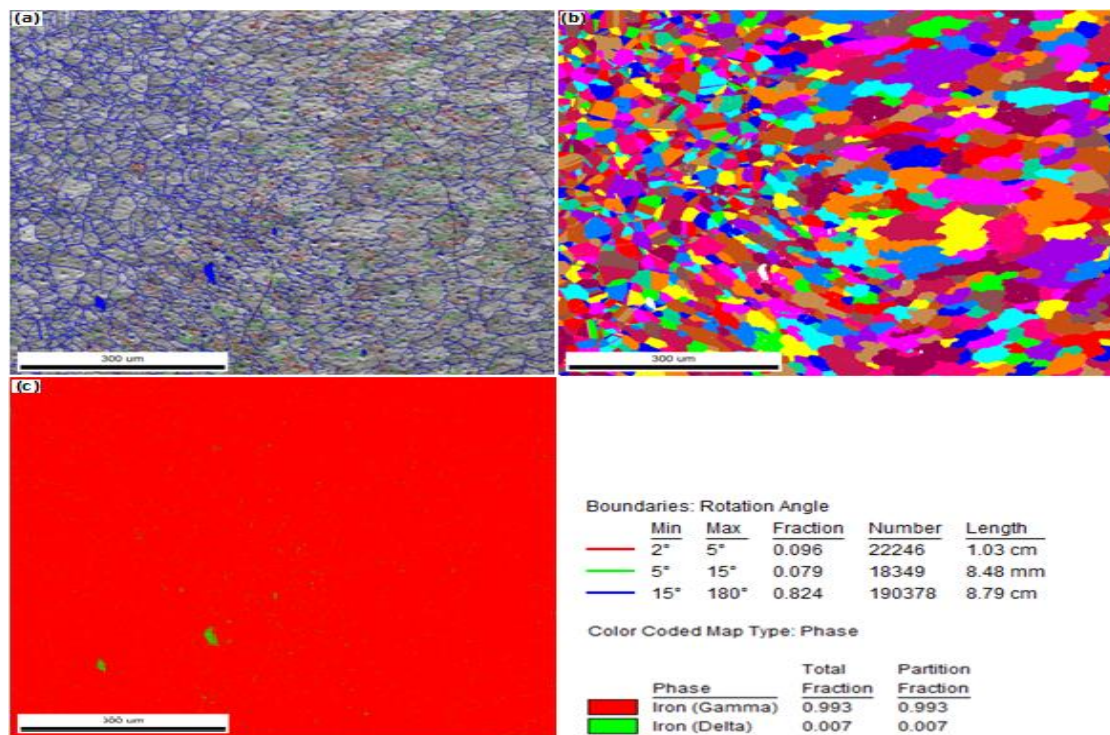


Fig.9 Grain orientation, OIM maps and phase analysis maps for weld interface of high nitrogen stainless steel SMA welds

Table 3 Percentage of ferrite, Grain Size, Mis-orientation angle and hardness of high nitrogen stainless steel SMA welds

Name	Surface δ ferrite (%)	Austenite (%)	Average Grain Size(μm)	Average Mis-orientation Angle($^{\circ}$)	Vickers Hardness (VHN)
Base Metal	1.7	98.3	3.7	46	410
Fusion Zone	0.4	99.6	33.8	28	228
Interface/HAZ	0.7	99.3	15.6	37	266

3.2 Mechanical properties

Nitrogen being a strong austenite stabilizer and reduces the requirement of nickel and improves microstructural stability and resistance to deformation induced martensite. Improvement in strength of high nitrogen stainless steel is influenced by solid solution hardening and decrease in stacking fault energy [10]. In nickel free high Cr-Mn-N steels, decrease in stacking fault energy enhances formation of mechanical twins that enhances strength. Nitrogen containing austenitic stainless steels show high impact toughness and is attributed to the fact that nitrogen does not induce void nucleation sites in the steel [11]. However, increasing nitrogen content enhances strength and retains impact toughness. Hence, nickel free high nitrogen austenitic stainless steels have the optimum combination of strength, ductility and toughness. The high hardness values are observed in high nitrogen austenitic stainless steel when compared to the weld zone as shown in Fig.10 and given in Table 3. The grain refinement

and high strengthening effects could be attributed to increasing interstitial nitrogen content due to solid solution hardening and grain boundary hardening whereas coarse grains of the weld zone resulting in lower hardness values. Welding process may influence the mechanical properties of high nitrogen steel significantly. Factors like heat input, cooling rate, electrode/filler wire composition leads to microstructural changes due to varying thermal cycles in the weld joints. Figs. 11-12 shows the failure location, stress-strain curve and FESEM fractograph of base metal and SMA welds. Table 4 contains tensile properties of base metal in comparison to the welds. SMA welds were observed to have less tensile strength when compared to base metal and is attributed to coarse grained and dendritic cast structure in the weld metal. Ductile fracture morphology with some fine dimples was observed. Face bend ductility tests revealed ductile joints and did not fail even for bending at 180° at a bend radius of 16mm as shown in Fig.13.

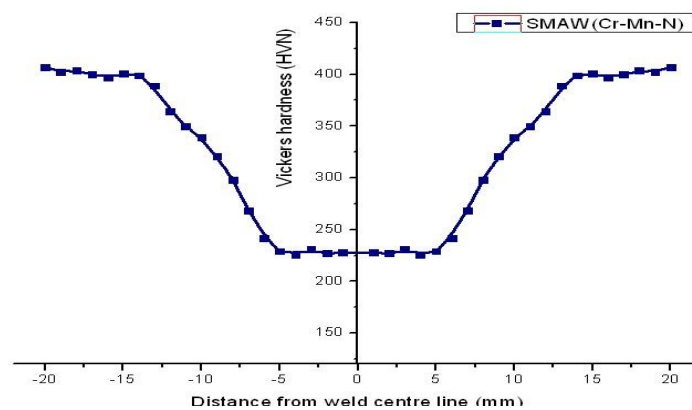


Fig. 10 Vickers hardness survey for SMA welds of high nitrogen stainless steel

Table 4 Tensile properties and impact toughness of shielded metal arc welds of nickel free high nitrogen stainless steel

Material	0.2% YS (MPa)	UTS (MPa)	El (%)	Location of failure
HNS (Base)	1190	1215	22	Centre
Cromang-N electrode	233	677	8.4	Weld region

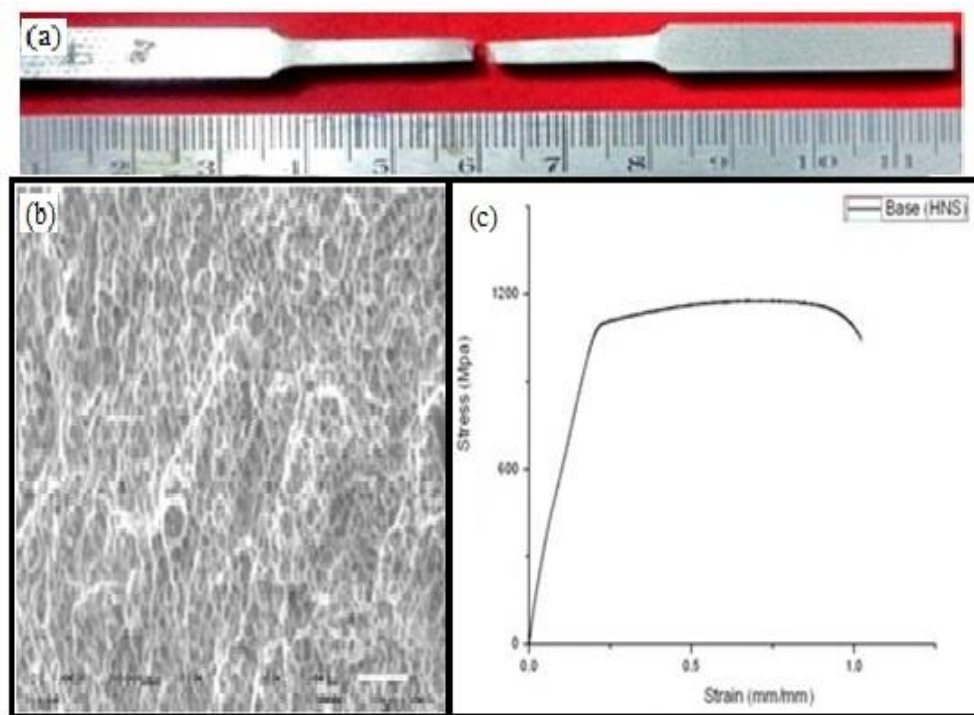


Fig. 11 Fracture features of tensile specimens of nickel free high nitrogen stainless steel (a) tensile failed specimen (b) stress-strain curve and (c) SEM fractograph

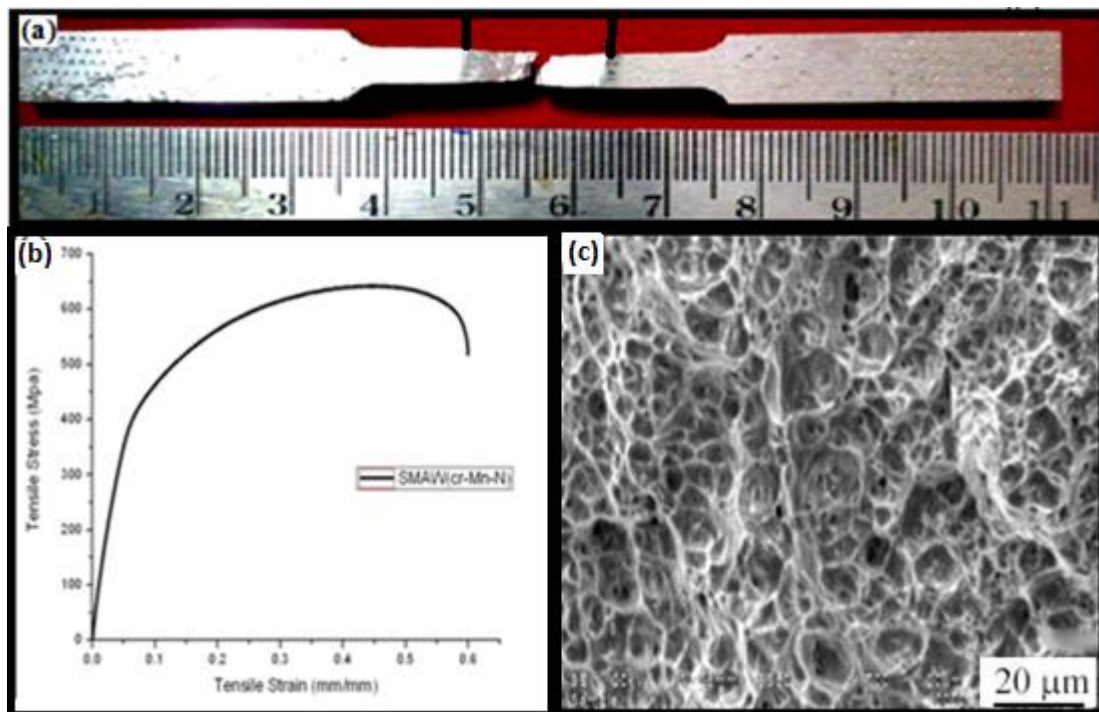


Fig. 12 Fracture features of tensile specimens of SMA welds of nickel free high nitrogen stainless steel with Cromang-N electrode (a) tensile failed specimen (b) stress-strain curve and (c) SEM fractograph



Fig. 13 Face bend ductility test specimens of shielded metal arc weld of nickel free high nitrogen stainless steel

3.3 Pitting corrosion

Fig. 14 shows the potentiodynamic polarization curves for SMA welds made using Cromang-N electrode in 3.5% NaCl solution using a basic electrochemical cell. The pitting potential (E_{pit}) of the weld metal is found to be 270 mV and observed to be more positive than base metal (130mV). SMA weld metal has better corrosion resistance compared to base metal which is attributed to the single phase austenite and coarse dendritic microstructure. The lower pitting corrosion resistance is observed in the weld metal interface region (55mV) when compared to that of base metal and weld metal. Corrosion potential, composition of the alloy, grain size of the welds affects the corrosion behaviour. Pitting corrosion of high nitrogen stainless steel and its welds has been found to be sensitive to microstructure. Relatively lower pitting potential was observed at the weld interface of SMA weld. Since weld interface acts as anodic and preferential pit initiates in this region when compared to weld metal and base metal.

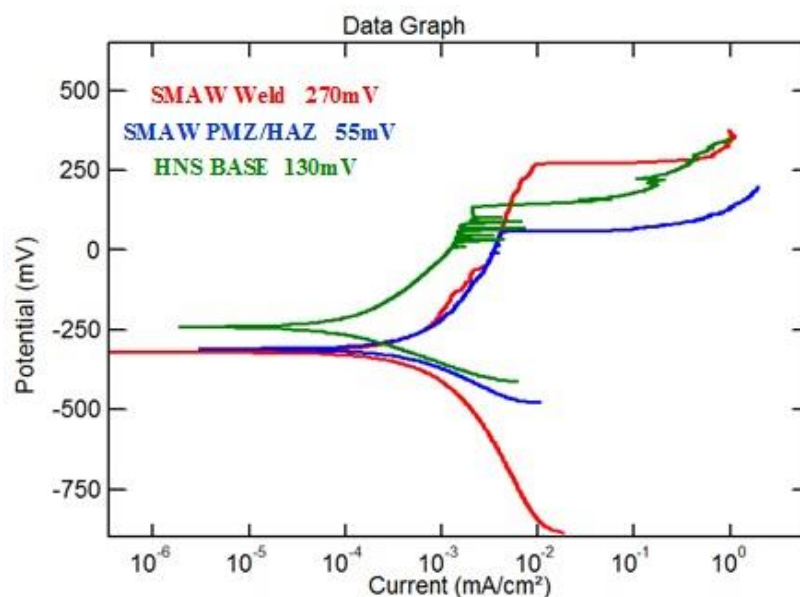


Fig 14 Potentiodynamic polarization curves of high nitrogen stainless steel shielded metal arc weld made with Cromang-N electrode

3.4 Stress corrosion cracking

The SCC test was carried out using smooth tensile flat specimen and Fig.15a shows the SCC failed test specimen of high nitrogen stainless steel. Stress corrosion cracking testing of base metal and SMA welds was carried out with a constant load type SCC machine with a fabricated cell loaded with 50% yield stress of the material and tested in a more aggressive environment of 45% MgCl_2 solution boiling at 155°C and studied by recording the “stress-time curves”. Failure occurs due to the synergistic action of tensile stress, corrosive environment and susceptible microstructure [12]. Time to failure of base metal and SMA weld was considered to observe the stress corrosion cracking resistance. High nitrogen stainless steel is prone to stress corrosion cracking and susceptible to magnesium chloride environment and is due to decreased amount of ferrite. The failed test specimen is shown in Fig. 15a and stress-time curve is given in Fig. 15b. Failure time was found to be 25 hours and given in Table 5. SEM fractograph is as shown in Fig. 15c clearly reveals the mixed mode of failure with multiple cracks. Fig. 16a shows the SCC failed test specimen of SMA weld and stress-time curve was shown in Fig. 16b. Failure time is found to be 42 hours. Fractograph as shown in Fig. 16c clearly reveals the attack in the weld interface region. SCC test data is given in Table 5. Failure can be correlated to observe microstructural changes and relative lower pitting potential in the weld interface. Preferential attack initiates in the weld interface region as it is having lower pitting potential active site for anodic dissolution when compared to weld metal and base metal. Hence, it is observed that weld metal of shielded metal arc (SMA) welds made with Cromang-N type electrode is having higher pitting potential when compared to base metal and weld interface.

Table 5 Stress corrosion cracking testing data of high nitrogen stainless steel and SMA welds

Material	Applied Stress (50% Y.S)	Environment	Failure location	Time to Failure, t_f
HNS	595 MPa	45% MgCl_2	Centre	25 Hours
Cromang – N	117 MPa	45% MgCl_2	Weld interface	42 Hours

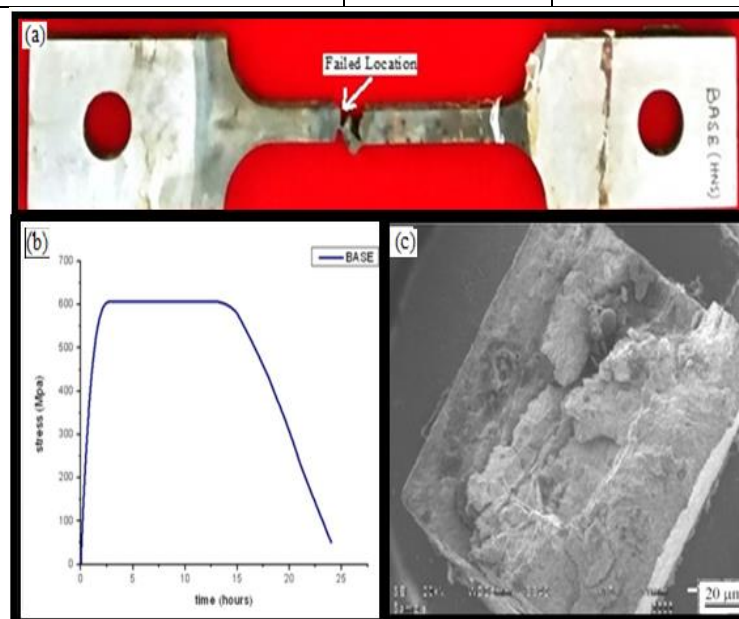


Fig 15 Stress corrosion cracking test specimen of nickel free high nitrogen stainless steel (a) failed SCC specimen (b) stress-time curve and (c) FESEM fractograph

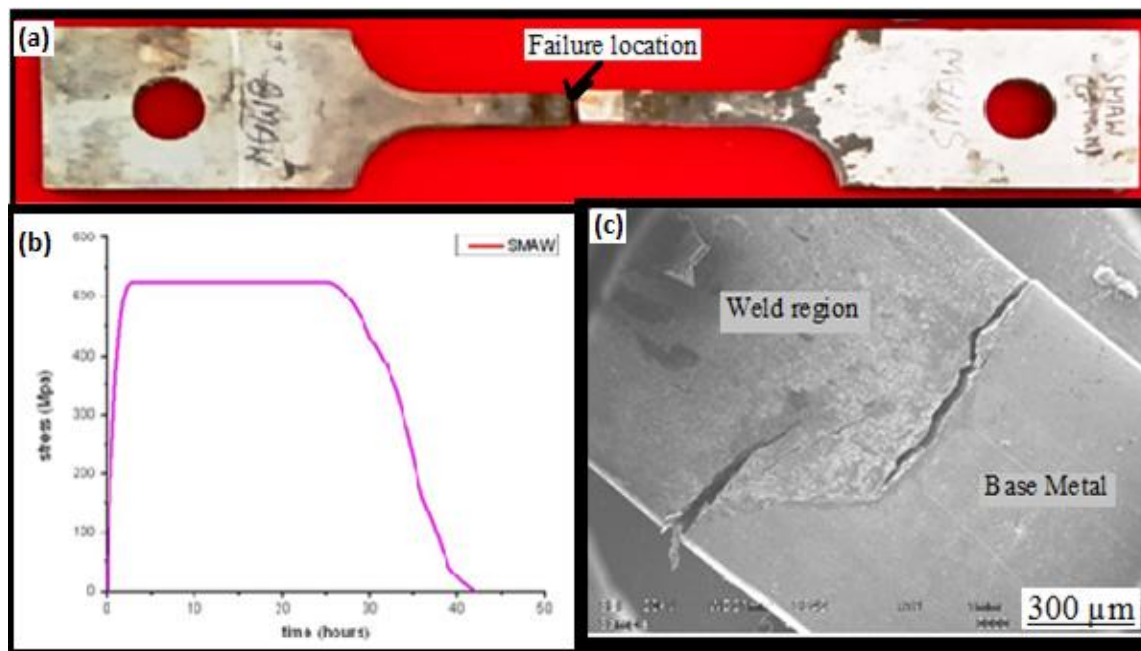


Fig. 16 Stress corrosion cracking test specimen of nickel free high nitrogen steel shielded metal arc welds made with Cromang-N electrode (a) Failed SCC specimen (b) Stress-Time curve and (c) FESEM Fractograph

Conclusions

1. Use of Cromang-N type electrode in shielded metal arc welding of high nitrogen steel resulted in defect free and sound welds. Electrode composition alters the microstructure of weld metal and weld interface regions.
2. Microstructure of the high nitrogen stainless steel is having single phase austenite microstructure with annealing twins in the base metal whereas weld metal of high nitrogen steel SMA welds was observed to be solidified as coarse dendritic austenite.
3. Relatively lower mechanical properties were observed for high nitrogen stainless steel SMA welds when compared to base metal and it is due to coarser and dendrite structure.
4. Improvement in pitting potential is observed in the weld metal when compared to weld interface and base metal. It is attributed to the coarse austenite grains owing to the reduction in active sites of the austenite/delta ferrite interface and decrease in galvanic interaction between austenite and delta-ferrite.
5. SCC failure time significantly improved for high nitrogen stainless steel SMA welds when compared to base metal but failure was observed in the weld interface region. Preferential attack initiates in the weld interface which acts as anodic and due to lower pitting potential when compared to weld metal and base metal.

Acknowledgements

The authors would like to thank Director, Defence Metallurgical Research Laboratory, Hyderabad, India for his continued encouragement and permission to publish this work.

References

- [1] Garner F A, Brager H R, Gelles D S and Mc Carthy J M: *J. Nucl. Mater.* 148 (1987), pp. 294.
- [2] Hosoi Y, Okazaki Y, Wade N and Mytyabara K *J. Nucl. Mater.* 169 (1989), pp. 257.

- [3] Madeleine du Tolt, *J. Mater. Engg & Perf.* (2002) 11: pp. 306-312.
- [4] Baldev Raj, P.Shankar and T Jayakumar, *Advances in Stainless Steel.* (2010) pp. 342.
- [5] Kotecki D J and Sievert T A, *Weld. J.*(1992) pp. 171-78
- [6] Honeycombe J and Gooch T G, *Metal Constr. & B. Weld. J.* (1972) pp. 456-60.
- [7] Parvathavarthini N, Dayal R K, Seshadri S K, Gnanamoorthy J B, *J.Nucl.Mater.* (1989) pp. 83.
- [8] Yao Fu, Xinqiang Wu, En-Hou Han, Wei Ke, Ke Yang, Zhouhua Jiang, *J. Electrochemical Acta.* (2009) pp. 1618-1629.
- [9] Nage Deepashri D, Raja VS. Effect of nitrogen addition on the stress corrosion cracking behavior of 904 L stainless steel welds in 288°C deaerated water. *J Corrosion Science*, 48, (2006), pp. 2317-31.
- [10] Mathew M D, Srinivasan V S, Mechanical properties of nitrogen bearing steels Monograph on High Nitrogen Austenitic Steels and Stainless Steels, Kamachi Mudali U and Baldev Raj (Eds.), Narosa Publications, New Delhi, (2004) 82.
- [11] Speidel M O, *proc. Of Intl. Conf. On high nitrogen steels*, HNS 88 (1989) 92.
- [12] Trethewey K R, Some observations on the current status in the understanding of stress-corrosion cracking of stainless steels, *Materials and Design*, 29, (2008), pp. 501-507.